IEEE Access
Multidisciplinary | Rapid Review | Open Access Journal

SPECIAL SECTION ON COLLABORATIVE INTELLIGENCE FOR INTERNET OF VEHICLES

Received July 9, 2021, accepted August 3, 2021, date of publication August 18, 2021, date of current version August 27, 2021.

Digital Object Identifier 10.1109/ACCESS.2021.3105750

Spatiotemporal D2D Small Cell Allocation and On-Demand Deployment for Microgrids

HAO RAN CHI[1], (Member, IEEE), MARIA DE FÁTIMA DOMINGUES[1], (Member, IEEE), KONSTANTIN. I. KOSTROMITIN[2], AHMAD ALMOGREN[3], (Senior Member, IEEE), AND AYMAN RADWAN[1], (Senior Member, IEEE)

[1]Instituto de Telecomunicações and Universidade de Aveiro, 3800-193 Aveiro, Portugal
[2]Department of Physics of Nanoscale Systems, South Ural State University, 454000 Chelyabinsk, Russia
[3]Department of Computer Science, College of Computer and Information Sciences (CCIS), King Saud University (KSU), Riyadh 11633, Saudi Arabia

Corresponding author: Ayman Radwan (aradwan@av.it.pt)

This work was supported in part by the FCT/MCTES through national funds, in part by the EU funds under Project UIDB/50008/2020-UIDP/50008/2020, in part by the Internal Project X-0005-AV-20-NICE-HOME, and in part by King Saud University, Riyadh, Saudi Arabia, under Researchers Supporting Project number RSP-2021/184. The work of Maria de Fátima Domingues was supported in part by the Scientific Action REACT, and in part by FEDER–PT2020 Partnership Agreement under Project UID/EEA/50008/2019 FCT. The work of Ayman Radwan was supported by FCT/MEC through Programa Operacional Regional do Centro and by the European Social Fun (ESF) under Investigador FCT Grant 5G-AHEAD IF/FCT - IF/01393/2015/CP1310/CT0002.

ABSTRACT Microgrids in smart grid development create a new era towards resilient energy supply. In turn, They also render complicated cyber-physical system development towards high scalability and comprehensiveness. Heterogeneous Small Cell based Networks (HSCNs) endow a suitable cyber infrastructure for microgrid based cyber-physical systems. To tackle this emerging research area, this paper proposes a **S**patiotemporal **D**evice-to-device communication based H**S**CN **D**eployment scheme for Microgrid based **S**mart grid **D**evelopment (3xSD), to achieve high energy efficiency with high quality-of-service, chronically and dynamically. Concretely, a joint optimization for long-term energy efficiency and achievable data rate maximization with interference mitigation is formulated for spatial small cell positioning, which models both cyber and physical characteristics of Smart Grid User Equipment (SGUE). A Temporal On-demand Small cell Powering and work-Offloading scheme (TOSPO) is proposed on top of the determined small cell positioning. TOSPO considers the real-time heterogeneous features and demands of SGUEs to maximize energy and cost efficiency, for both communication and computation perspectives. To evaluate the performance of 3xSD, spatial analysis, temporal analysis, and selected case study are simulated. Numerical results showcase that 3xSD is capable of providing both long-term and on-demand optimal energy efficiency and quality-of-service solution for microgrids, outperforming existing benchmarks in the literature.

INDEX TERMS Small cells, smart grid, on-demand, energy efficiency, cyber-physical systems.

I. INTRODUCTION

Gaining an annual growing rate as 14% with more than 27 power capacity worldwide [1], microgrids have been playing an important role on the advanced smart grid development, capable of managing local energy resources and distributed power systems resiliently for critical communities [2]. As a typical cyber-physical system (CPS), prospective exceptional performance of microgrids is constructed upon the optimal deployment of communication technologies [3]–[5]. Heterogeneous Small Cell Networks (HSCNs) potentially manage the densification of Smart Grid User Equipment (SGUE) [6], [7] highly demanded by microgrids. Besides, Mobile Edge Computing embedded Small Cells (MEC-SCs) realize the distributed computation capacity for microgrid management [8]–[10], which will dominate the cyber system deployment [11]–[13].

Optimal HSCNs lead to high energy efficiency and high Quality-of-Service (QoS) at low costs, which are leading concerns to service providers for microgrids [1], [14]; however, MEC-SC based HSCN deployment for microgrids embraces a plethora of challenges. Firstly, with the popularization of microgrids, the scalability of HSCNs should be improved [15]. SGUEs are located in multiple

The associate editor coordinating the review of this manuscript and approving it for publication was Celimuge Wu.

microgrids and gain more diverse operation modes, e.g., periodic vs. non-periodic, large data rate demand vs. high reliability, etc., which complicates the cyber modeling of HSCN deployment. In particular, the popularity of Device-to-device (D2D) communications in HSCN deployment enable direct data transmission between two SGUEs, without going through SCs, which occurs due to the requirement of either direct communication between SGUEs (e.g., inner-mirogrid), or offloading among SGUEs for data relay, not necessarily at cell boundaries. Therefore, D2D modeling at the cyber layer might encounter unique features, brought by the cluster-based microgrids at the physical layer, requiring research efforts fusing cross-layer modeling [3], [16].

Besides, HSCN deployment should be optimized in both spatial and temporal ways, by achieving chronic and dynamic optimum, respectively. For instance, stochastic geometry based algorithms are considered recently as the backbone of spatial HSCN deployment [17]. However, previous works either build based on the assumption of full buffer [15] or statistic-based estimation [18], which fails to handle the real-time QoS optimization. It even deteriorates, when these previous works tackle real-time resource allocation for mirogrid based MEC-SC deployment. In contrast, some other cluster of researches perform real-time resource allocation, assuming optimal spatial HSCN allocation predetermined [19]. Therefore, spatiotemporal HSCN deployment is extremely necessary for comprehensive optimization in network automation in future communication networks (e.g., 6G) [20], [21], for microgrid based smart grid. Comprehensive spatiotemporal optimization of HSCN deployment also prevents potential cascading failure caused by deploying spatial and temporal HSCNs, separately. To the best of our knowledge, there is a lack of comprehensive studies on spatiotemporal HSCN deployment for microgrids.

In this paper, we tackle the aforementioned challenges by proposing a **S**patiotemporal **D**2D **S**mall-cell **D**eployment for microgrid based **S**mart-grid **D**evelopment, named as Triple-SD (3xSD). Concretely, the spatial Small Cell (SC) positioning scheme is proposed with VIKOR-based joint optimization of long-term energy efficiency optimization, achievable data-rate maximization and interference minimization. Extending the work in [3], the proposed spatial SC positioning scheme further models the SGUEs' physical and cyber functionalities, with the formulation of model-driven communication and computation processes. On top of the SC positioning scheme, a Temporal On-demand SC Powering and work-Offloading scheme, named TOSPO, achieves data-driven energy and cost efficiency management dynamically, by k-means clustering SC powering and gradient descent based MEC-SC work offloading. The contributions of this paper are summarized, as follows:

1. We propose a spatiotemporal D2D HSCN for microgrid based smart grid development (3xSD) with long-term and real-time energy efficiency and Quality-of-Service (QoS) optimized, simultaneously.

2. We develop a VIKOR-based SC positioning for long-term energy efficiency and achievable data rate maximization with interference mitigation, considering the model-driven SGUE formulation.

3. We propose a Temporal on-demand MEC-SC Powering and work Offloading scheme (TOSPO) for real-time overall latency minimization and energy efficiency maximization, based on k-means clustering and gradient descent algorithm, respectively.

The rest of the paper is organized as follows: Section II reviews the related works. Section III overviews the proposed 3xSD infrastructure. Section IV derives the spatial SC positioning scheme with network modeling and optimization formulation. Section V proposes the on-demand SC deployment scheme (TOSPO), with k-means clustering based SC powering and gradient descent MEC-SC work offloading. Section VI analyzes the performance of 3xSD using simulations. Section VII concludes.

II. RELATED WORK

Microgrid based smart grid, regarded as a typical CPS, gains great research attention for the deployment of both physical (power systems) and cyber (communication networks) layers, as well as the harmonization between them, aiming to improve resilience and cost efficiency simultaneously [22]–[25]. Distributed energy management schemes, e.g., optimal power flow [23], were proposed regarding the physical requirements from power systems. However, objectives, such as cost efficiency in this research cluster, were modeled based on the physical layer of microgrids [26]. For instance, topological analysis for the optimal power flow was conducted, with the association between devices determined by power grid (e.g., the minimum power lost on power lines) [23]. A real-time pricing strategy was also proposed for SG based on the green IoT [27], which concentrated on the physical layer modeling, assuming the cyber layer to be optimally designed. On the other hand, although HSCNs have been popularized in 5G cellular networks to support large scale CPSs, characteristics of users/devices in the physical layer were mostly neglected [15], [28]. For instance, energy efficiency management of HSCNs was tackled with energy harvesting, based on sleeping strategies of SBSs [8], [28], which modelled the traffic flow as constant statistical traffic pattern affected by the cyber layer.

Moreover, a plethora of researches achieved delay minimization [29], QoE improvement [30], and energy efficiency maximization [19], [31], for HSCN deployment. However, these efforts mostly ignored the spatial SC allocation, which might cause unnecessary long-term cost waste, with inter-cell interference problems and QoS reduction. One of the main reasons for ignoring spatial SC allocation resulted from the concentration on small-scale networks considering single- or bi-SC modeling and analysis [32], which might not be applicable for large-scale smart grid.

The activation of MEC-SCs complicates the HSCN deployment with resource allocation among distributed

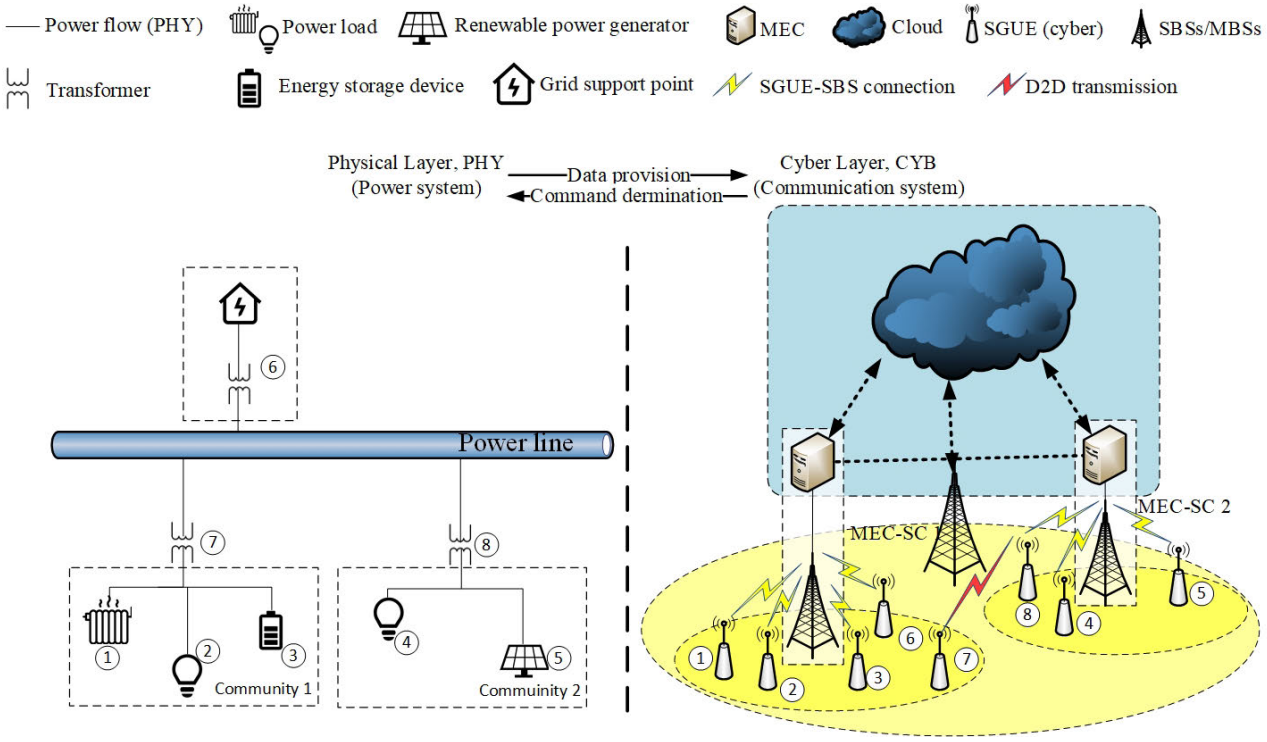

FIGURE 1. Infrastructure of the proposed 3xSD.

computing units [8], [33]. As an emerging technology, MEC-SCs highly demand work offloading strategies to optimize the communication and computation quality. Because of the formulation complexity, MEC-SC work offloading schemes normally adopted heuristic algorithms (e.g., genetic algorithm [6], bender decomposition [34]). These algorithms either significantly worsened the latency performance with tedious solution searching processes, or complicated algorithm parameter determination (e.g., maximum iteration, population size, etc.); the improper design of which directly resulted in failure to find optimum solution. Deterministic algorithms (e.g., ADMM) were considered, which normally sacrificed the formulation accuracy (e.g., by discarding coupling parameters in the constraints [35]). Besides, as aforementioned, the spatial SC allocation, together with microgrid customization in the system modeling, was not considered in these works.

A joint optimization of data rate maximization and interference mitigation was proposed [3], which provided a generic spatial SC allocation for SG. Nevertheless, to maximize the QoS performance, energy efficiency was not emphasized, which was one of the main blocks to service providers for the popularization of microgrids. Features of SGUEs were also not comprehensively modeled in the optimization process, with transmission pattern assumed as homogeneous and communication/computation resources as sufficient. Therefore, in this paper, we fill in the research gap and extend the research scope, to propose a spatiotemporal D2D based HSCN deployment for microgrids.

There are several spatiotemporal systemic deployment schemes proposed previously [17], [18], [36]–[40], which have pointed out the limitations of separately handling either spatial deployment or real-time resource allocation. spatiotemporal SINR analysis was conducted for HSCNs, trying to overcome the limitation of modeling bias caused by full buffer assumptions in stochastic geometry based spatial allocation [40]. Besides, delay analysis was also provided for 5G networks, effectively modeling delay throughout physical and application layers [39]. However, although raising up the importance of systemic spatiotemporal analysis, the abovementioned works might fail to be applied in MEC-SC based HSCN deployment for microgrids, with D2D activated, rendering lack of customized system modeling.

Comparison between the proposed 3xSD and selected literature survey is summarized in TABLE 2, to elaborate on the paper's innovations.

III. INFRASTRUCTURE OF SPATIOTEMPORAL MEC-SC DEPLOYMENT FOR MICROGRID BASED SMART GRID (3xSD)

In this paper, SG is upgraded by microgrids with the full utilization of the distributed power supports, achieving higher energy efficiency and low cost in the future distributed SG development [23]. Based on the natural features of microgrids, Figure 1 shows the infrastructure of the proposed 3xSD, divided and interacted by physical and cyber layers. We assume that N SGUEs are served, which contributes to N devices in the power system and N end devices in the communication system, simultaneously, by assuming each SGUE

TABLE 1. Key abbreviations and notations.

Acronym	Description	Acronym	Description
HSCN	Heterogeneous small cell networks	M	No. of MEC-SCs
3xSD	**S**patiotemporal **D**2D based HSCN **D**eployment scheme for microgrid based **S**mart grid **D**evelopment	$a_{mn}(t)$	Association between SC m and SGUE n
D2D	Device-to-device communications	$\tilde{E}$	Energy efficiency
SGUE	Smart grid user equipment	$\tilde{\gamma}_m$	SINR of SBS m
CPS	Cyber physical system	$\tilde{x}$	Estimated formulation of parameter x
TOPSO	Temporal on-demand small cell powering and work-offloading scheme	$N'_m(t)$	No. of active SGUE at time t
SC	Small cells	E_{cp}^{MEC-SC}	Computation power consumption
MEC-SC	Mobile edge computing based SC	D_{cp}^{MEC-SC}	Computation latency
QoS	Quality of service	N	No. of SGUEs
SBS	SC based base station	$c_{mn}(t)$	Physical coverage of SC m
MBS	Macro-cell based base station	S_i	Functionality
SINR	Signal to noise ratio	L_n	Location of SGUE n
$\vartheta_n(t)$	D2D activation of n at time t	$tr_{S_i}(t)$	Transmission pattern of S_i at time t
σ_{mn}	Throughput between m and n	$\varphi_m(t)$	Activation of SC m

TABLE 2. Comparison between the proposed 3xSD and previous works.

Features	[1]	[4]	[18]	[22]	[24]	[31]	[38]	[39]	3xSD
Physical system modeling	N	Y	N	N	N	N	N	N	Y
Cyber system modeling	Y	N	Y	Y	Y	Y	Y	Y	Y
Spatial SC allocation	Y	N	N	N	N	N	N	N	Y
Real-time operation	N	Y	Y	Y	Y	N	Y	Y	Y
Communication modeling	Y	N	Y	Y	Y	Y	Y	Y	Y
Computation modeling	N	N	Y	N	N	N	Y	N	Y
Large-scale	Y	Y	N	Y	N	N	Y	Y	Y
Deterministic	N	Y	Y	N	N	Y	N	N	Y
QoS considered	Y	N	Y	Y	Y	N	Y	Y	Y
Energy efficiency optimized	N	Y	Y	Y	N	Y	N	N	Y
Interference mitigated	Y	N	N	N	Y	N	Y	Y	Y

embedded with one transceiver. M MEC-SCs are deployed to provide efficient connectivity and distributed computation capacity for SGUEs in the coverage of a macro-cell, with the value M and corresponding MEC-SC locations and operations (e.g., powering, work offloading) to be determined by the proposed 3xSD. The SGUEs select a serving SC base station (SBS) with maximum reference signal received power (RSRP), or route their data to neighboring SGUEs, according to D2D based multi-hop communications. Macro-cell base stations (MBSs) are mainly responsible for coordinating SBSs with work offloading commands, communicating with cloud servers, and providing propagation flow to SGUEs uncovered by SCs.

Physical layer (PHY), i.e., power systems in microgrids, consists of traditional power generators, distributed renewable power generators, power loads and energy storage devices [1]. Abundant SGUEs within multiple microgrids render various service demands. At PHY layer, SGUEs are assigned with the following parameters:

1. Functionality: SGUEs can be classified as traditional generators (S_g), renewable generators (S_r), power loads (S_l), and energy storage devices (S_e), respectively, which gains high diversity on the power transfer and communication patterns in 3xSD. For instance, S_g normally requires regular data aggregation and analysis to implement a regular optimal power flow management [41], whereas S_e may be equipped with event-triggering transceivers to dynamically reporting the charging/ discharging demand and situation [22].

2. Locations: Because PHY defines the services in microgrids, the location of SGUEs should be assigned according to their requirements from the power system, which is derived as:

$$L_n = (x_n, y_n), \quad n \in \{1..N\} \tag{1}$$

where x_n and y_n are the axis of SGUE n, according to the x-y spatial distribution. It is necessary to mention that the location of SGUEs are normally stabilized temporally, with SGUEs normally installed fixedly.

3. Microgrids: The microgrid that SGUE n belongs to is derived as $C_n, n \in \{1..N\}$. In general, SGUEs in the same microgrid might suffer from less privacy issues, meanwhile data shared in the same microgrid can achieve high efficiency, according to the short physical distance. Moreover, D2D could be activated more securely among SGUEs in the same microgrid.

Cyber layer, which is the communication networks (i.e., HSCN) served in microgrid, also defines SGUEs in communication and computation perspectives, including:

1. Transmission pattern: As mentioned, SGUEs require periodic or non-periodic data transmission, according to their unique $S_i, i \in \{g, r, l, e\}$ in the power system. Therefore, transmission patterns of SGUE n in the cyber layer, $tr_n(t), n \in \{1..N\}$, can be either 1 or 0, representing periodic and non-periodic, respectively, at time t.

2. D2D activation: D2D is activated for SGUE n when data relay among SGUEs is necessary, with its D2D mode defined with $\vartheta_n(t) = 0, n \in \{1..N\}$ as not activated and $\vartheta_n(t) = 1$ as activated at time t. Correspondingly, the D2D activation between two SGUEs, n and o, is derived as

$$\theta_{no}(t) = \begin{cases} 1, & activated \\ 0, & otherwise, \end{cases} \quad n, o \in \{1..N\} \tag{2}$$

3. SC coverage: $c_{mn}(t), m \in \{1..M\}, n \in \{1..N\}$ is defined as the physical coverage of SCs, regarding to SGUEs, based on the potential link budget between SCs and SGUEs. $c_{mn}(t) = 1$ indicates that the transmit power of SC m is sufficient to support the data propagation to/from SGUE n.

4. SGUE-SC association: $a_{mn}(t), m \in \{1..M\}, n \in \{1..N\}$ is defined as 1 when connected and 0 otherwise. It is necessary to mention that with the activation of D2D, $a_{mn}(t)$ does not necessarily mean SGUE n is physically covered by SC m, which could relay its data via D2D. Detailed principles and relationship between $c_{mn}(t)$ and $a_{mn}(t)$ are illustrated in Section III.B.

It is intuitive that S_i, L_n and C_n $(i \in \{g, r, l, e\}, n \in \{1..N\})$ are defined when initializing 3xSD and temporally stable, whereas $tr_n(t)$, $\vartheta_n(t)$, $\theta_{no}(t)$, $c_{mn}(t)$ and $a_{mn}(t)$ $(m \in \{1..M\}, n \in \{1..N\})$ are temporally dynamic, which should be predicted/measured in the spatial/temporal deployment of the proposed 3xSD, respectively. Moreover, the hypotheses that the proposed 3xSD makes are summarized as:

Hypothesis 1: *Each SGUE $n \in \{1..N\}$ is associated with one and only one SC m (where $m \in \{1..M\}$), at time t, either directly covered by SC m or by D2D:*

$$\forall n \in \{1..N\} : \sum\nolimits_{m \in \{1..M\}} a_{mn}(t) = 1 \tag{3}$$

Hypothesis 2: *To prevent latency performance affected by multi-hop communication, when D2D activated at time t for SGUE n, data can be relayed to one and only one SGUE:*

$$\forall \vartheta_n(t) = 1 : \sum\nolimits_{o \in \{1..N\}} \theta_{no}(t) = 1, \quad n \in \{1..N\} \tag{4}$$

IV. SPATIAL SC POSITIONING

In this section, we propose the spatial deployment of 3xSD, which optimally determines the SC positioning. It is necessary to note here that SGUEs are already registered with their temporally stabilized variables, e.g., S_i, L_n and G_n $(i \in \{g, r, l, e\}, n \in \{1..N\})$, as aforementioned. However, the dynamic variables of SGUEs should be estimated, represented by the statistical model-driven modeling, to provide a long-term energy-efficient SC positioning, meanwhile ensuring potential QoS performance optimized and interference mitigated.

A. VARIABLE ESTIMATION OF SGUES

Spatial HSCN deployment determines the SC positioning, including the number and positions of SCs. Excessive number of SCs increases the construction and operational costs, as well as reducing the energy efficiency, whereas the positions of SCs directly affect the inter-cell interference and the link budget of SGUEs. Therefore, energy efficiency maximization and estimated QoS should be considered, when optimizing the SC positioning in the spatial HSCN deployment, with interference mitigated.

Since D2D is activated, SGUE n could have two possible data transmission paths. One is directly connected with one SBS via the coverage of one SC with sufficient link budget. The other could transmit via D2D, by relaying data to the adjacent SCs (not physically covered). These two paths correspond to the determination of the D2D activation defined in Section III, with $\vartheta_n(t) = 0$ and 1 $(n \in \{1..N\})$, accordingly. In addition, SGUE data transmission path could also determine $c_{mn}(t)$ and $a_{mn}(t)$ $(m \in \{1..M\}, n \in \{1..N\})$, with the properties defined as:

Property 1: $\forall t \in [0, T]$, *if* $\vartheta_n(t) = 0 \& c_{mn}(t) = 1$, $a_{mn}(t) = 1$, *based on Hypothesis 1.*

Property 2: $\forall t \in [0, T]$, *if* $\vartheta_n(t) = 1 \& c_{mn}(t) = 0$, $a_{mn}(t) = 0$, *based on Hypothesis 1.*

Property 3: $\forall t \in [0, T]$, $\vartheta_n(t) + c_{mn}(t) = 1$.

Properties 1-3 can be further derived, with the definition of $\theta_{no}(t)$ $(n, o \in \{1..N\})$:

Property 4: $\forall t \in [0, T]$, *if* $\vartheta_n(t) = 0$ *or* $\vartheta_o(t) = 0$, $\theta_{no}(t) = 0$, *according to (2);*

Property 5: $\forall t \in [0, T]$, *if* $\theta_{no}(t) = 1$, $\vartheta_n(t) = \vartheta_o(t) = 1$, *according to (2);*

Property 6: $\forall t \in [0, T]$, *if* $\vartheta_n(t) = \theta_{no}(t) = c_{po}(t) = 1$, $c_{pn}(t) = 1$.

The association between SGUEs and SCs ($a_{mn}(t)$), as well as the D2D activation ($\vartheta_n(t)$) are determined dynamically, which can only be estimated according to the model-driven formulation for the spatial HSCN deployment of 3xSD. Therefore, all the time-variant variables are estimated in this section, represented as $x(t) \to \tilde{x}$, e.g., $\vartheta_n(t) \to \tilde{\vartheta}_n$ $(n \in \{1..N\})$.

Based on the association of SGUE-SC, and D2D probability, the inter-cell interference in the spatial HSCN deployment of the proposed 3xSD is formulated related to the average

signal to interference-noise ratio (SINR), which is formulated in the point of view of SC m, as

$$\tilde{\gamma}_m(M, L_m) = \sum\nolimits_{n\in\{1..N\}} \frac{\tilde{P}_m \cdot G_{mn}}{N+\tilde{I}_{mn}} \cdot \tilde{c}_{mn} \cdot \tilde{a}_{mn}, \quad m \in \{1..M\} \tag{5}$$

where L_m is the location of the SBS m, which is one of the outputs of the spatial SC positioning scheme in 3xSD. $\tilde{P}_m$ is the transmit power of the SBS m, which is estimated as average of the solution space of transmit power. $G_{m,n}$ refers to the gain of the SBS m to SGUE n. $\tilde{\gamma}_m(M, L_m)$ is calculated with the estimation of D2D probabilities (estimated regarding L_n and C_n), by considering the estimated $\tilde{c}_{mn}$ and $\tilde{a}_{mn}$. N and $\tilde{I}_{mn}$ are the additive Gaussian noise and interference, respectively, with I_{mn} estimated as

$$\tilde{I}_{mn} = \sum\nolimits_{i\in\{1..M\}, i\neq m} \mathbb{E}\left[\tilde{P}_i \cdot G_{in} \cdot \tilde{h}_{in}(M, L_m)\right], \quad n \in \{1..N\} \tag{6}$$

where $\tilde{h}_{in}(M, L_m) \leftarrow h_{in}(M, L_m, t)$ is the estimated time-varying small-scale fading channel gain from SBS i to SBS m.

According to Shannon based capacity formula, the achievable throughput between SBS m and SGUE n is [6]:

$$\tilde{\sigma}_{mn}(M, L_m) = B_m \log_2\left(1 + \frac{\tilde{P}_m \cdot G_{mn}}{N + \tilde{I}_{mn}(M, L_m)} \cdot \tilde{c}_{mn} \cdot \tilde{a}_{mn}\right), \quad m \in \{1..M\}, n \in \{1..N\} \tag{7}$$

where B_m is the bandwidth available for the SBS m. Considering D2D communication, the overall achievable data rate of SBS m and energy efficiency ($\tilde{E}(M, L_m)$) estimated in the spatial tier are calculated as:

$$\begin{aligned} \forall m \in \{1..M\} : \tilde{\sigma}_m(M, L_m) &= \sum\nolimits_{n\in\{1..N\}} \sum\nolimits_{i\in\{1..M\}} \sigma_{in}(M, L_i) \cdot \tilde{\vartheta}_n \cdot \tilde{a}_{mn} \cdot \tilde{c}_{in} \\ &\quad + \sum\nolimits_{n\in\{1..N\}} \tilde{\sigma}_{mn}(M, L_m) \end{aligned} \tag{8}$$

$$\tilde{E}(M, L_m) = \sum\nolimits_{m\in\{1..M\}} \frac{\tilde{P}_m}{\tilde{\sigma}_m(M, L_m)} \tag{9}$$

B. SPATIAL SC POSITIONING SCHEME

In this paper, we maximize energy efficiency and achievable data rate with interference mitigation for HSCN by the spatial SC positioning, which ensures the optimal long-term HSCN deployment for microgrids, and thus paves the infrastructural way to the dynamic temporal HSCN deployment (i.e., TOSPO). Therefore, the optimization problem for spatial SC positioning is formulated as a conflictive multi-objective optimization based on (5), (8) and (9), with weighting factors assigned ($m \in \{1..M\}$):

$$\begin{aligned} F_{sp}(M, L_m) &= \omega_1 f_{sp,1}(M, L_m) + \omega_2 f_{sp,2}(M, L_m) \\ &\quad + \omega_3 f_{sp,3}(M, L_m) \\ &= \omega_1 \left\| \sum\nolimits_{m\in M} \tilde{\sigma}_m(M, L_m) \right\| + \omega_2 \left\| \tilde{E}(M, L_m) \right\| \\ &\quad + \omega_3 \left\| \sum\nolimits_{m\in M} \tilde{\gamma}_m(M, L_m) \right\| \end{aligned} \tag{10}$$

where $f_{sp,1}(M, L_m)$, $f_{sp,2}(M, L_m)$ and $f_{sp,3}(M, L_m)$ are the three objectives for the spatial SC positioning scheme, namely achievable data rate maximization, energy efficiency maximization, and interference mitigation (e.g., SINR maximization), respectively, which are normalized to be comparable. $\omega_1, \omega_2, \omega_3 \in [0, 1]$ are the weighting factors for the three objectives, which should be determined according to the demand of service providers of microgrid. For instance, for the microgrid serving hospitals, interference should be mitigated with less emphasis on energy efficiency to ensure the reliability of the HSCN. On the other hand, for commercial usage of microgrid, service providers might seek more cost-effective solution for the HSCN deployment to reduce cost.

The applicable constraints include (3)-(4), and (11)-(13) defined as the achievable data rate of each SGUE fulfilling microgrid demands, backhaul flow limit of each SBS, and transmit power limit for each SBS, respectively:

$$\tilde{\sigma}_{mn}(M, L_m) \geq \tilde{\sigma}_{mn}^{min}, \quad m \in \{1..M\}, n \in \{1..N\} \tag{11}$$

$$\tilde{\sigma}_m(M, L_m) \leq \sigma_m^{max}, \quad m \in \{1..M\} \tag{12}$$

$$\tilde{P}_m \in \left[0, P_m^{max}\right], \quad m \in \{1..M\} \tag{13}$$

It is obvious that the optimization problem (10), with the constraints, is highly non-linear mixed-integer programming. Instead of discarding or relaxing the integer variables [35], which might sacrifice the formulation accuracy, we develop a multi-criteria decision making algorithm based on VIKOR, a commonly-recognized optimization algorithm with fast computation and accuracy [42], to search for a trade-off solution for the multi-objective optimization problem of the spatial SC positioning scheme. The global best and worst values for all the objectives should be analyzed as $f_{sp,i}^*$ and $f_{sp,i}^-$, respectively, with $i \in \{1, 2, 3\}$ in the scheme. The utility measures (U) and regret measures (R) are further calculated for each candidate solution:

$$U_m = \sum\nolimits_{i\in\{1,2,3\}} \alpha_i \frac{f_{sp,i}^* - f_{sp,i}(m, L_m)}{f_{sp,i}^* - f_{sp,i}^-}, \quad m \in \{1..M\} \tag{14}$$

$$R_m = \max\left[\alpha_i \frac{f_{sp,i}^* - f_{sp,i}(m, L_m)}{f_{sp,i}^- - f_{sp,i}(m, L_m)}\right], \quad i \in \{1, 2, 3\}, \ m \in \{1..M\} \tag{15}$$

In this paper, to simplify the computation, the candidate solutions are selected based on M, while the corresponding location of SCs (L_m) is determined based on the principle that SCs should be located evenly to cover the serving space with minimum inter-cell interference. The global best and worst values of U and R, $\{U^*, U^-\}$ and $\{R^*, R^-\}$ are obtained similar to $\left\{f_{sp,i}^*, f_{sp,i}^-\right\}$. The sorting criteria ($S_m$) [3] with v generally set as 0.5 and the optimal solution by the spatial SC positioning scheme can be

obtained as

$$S_m = v\left(\frac{U_m - U^*}{U^- - U^*}\right) + (1-v)\left(\frac{R_m - R^*}{R^- - R^*}\right), \quad m \in \{1..M\} \tag{16}$$

$$M^{optimal} = \arg S_m \tag{17}$$

V. TEMPORAL ON-DEMAND SC POWERING AND WORK OFFLOADING (TOSPO)

The spatial SC positioning is determined in Section IV, with optimized long-term energy efficiency, maximized achievable data rate and mitigated inter-cell interference. However, real-time data-driven optimization process of HSCN deployment is still required to dynamically fulfill the demand of SGUEs, with real-time energy and cost efficiency management. Therefore, in this section, on-demand SC powering and offloading scheme (TOSPO) is developed for the temporal HSCN deployment of 3xSD.

A. ON-DEMAND MEC-SC POWERING STRATEGY

The dynamic MEC-SC powering scheme is proposed based on the sleeping strategy [28]. According to the heterogeneous operation modes of SGUEs, SBSs could fall into sleeping mode, when sufficiently few SGUEs are active in a time period, with the facilitation of D2D. According to the transmission pattern ($tr_n(t)$), SGUEs could be categorized as periodic and non-periodic, corresponding to the requirement from the physical layer of the proposed 3xSD.

The possibility that periodic SGUE n with the time interval T_n generates packets at the period Δt is formulated as

$$\delta_{tr_n(t)=1}(t) = \frac{\Delta t}{T_n}, \quad n \in \{1..N\} \tag{18}$$

Suppose there are n_m^p periodic SGUEs covered by SC m, with $c_{mn}(t) = 1, n \in \{1..n_m^p\}, , m \in \{1..M\}$, the number of active periodic SGUEs ($N_m^{p\prime}(t)$) and active non-periodic SGUEs ($N_m^{np\prime}(t)$) in SC m are derived based on (18) considering D2D, as

$$N_m^{p\prime}(t) = \sum\nolimits_{n\in\{1..n_m^p\}} \delta_{tr_n(t)=1}(t)\cdot a_{mn}(t) \tag{19}$$

$$N_m^{np\prime}(t) = \sum\nolimits_{n\in\{1..n_m^{np}\}} \delta_{tr_n(t)=0}(t)\cdot a_{mn}(t) \tag{20}$$

where $\delta_{tr_n(t)=0}(t)$ refers to the probability that non-periodic SGUE n will be active at $\{t, t+\Delta t\}$, which obeys the Poisson distribution. The total number of active SGUEs at time t is summed by (19) and (20) as

$$N_m'(t) = N_m^{p'(t)} + N_m^{np'(t)}, \quad n \in \{1..n_m^p\}, \ m \in \{1..M\} \tag{21}$$

Therefore, the clustering of active SGUEs at time t provides guidance to MEC-SC powering, intuitively by turning on MEC-SCs with large $N_m'(t)$, while switching MEC-SCs with less $N_m'(t)$ to sleeping mode and offload their work to adjacent MEC-SCs.

In the proposed TOSPO, we adopt k-means clustering for MEC-SC powering, which is capable of handling real-time MEC-SC powering with low computation costs, as a partitioned clustering algorithm. Besides, k-means clustering is applicable for SGUE clustering without outliers in microgrids, due to the physical close location of SGUEs in the same microgrid [1]. When initializing, the centroids of the cluster k ($\mu_k^0(t), k \in \{1..K\}$) at time t are randomly determined. All the other active SGUEs are clustered based on the minimum distance regarding $\mu_k^0(t)$ as:

$$k_n^0 = \arg\min_{k\in\{1..K\}} \left\| L_n - L^0_{\mu_k^0(t)} \right\|^2, \quad n \in \left\{1..n_m'(t)\right\} \tag{22}$$

For each iteration, the centroid is updated as the center of each cluster. The algorithm repeats until no SGUEs are re-assigned to other clusters, or the centroids are unchanged, or the sum of squared error decreases to the pre-defined level. The final centroid of clusters, $\mu_k^{i_{max}}(t), k \in \{1..K\}$, determines SC powering, with:

$$\tau_m(t) = \begin{cases} 1, & \sum_{k\in\{1..K\}} c_{m\mu_k^{i_{max}}(t)} = 1 \\ 0, & otherwise \end{cases}, \quad m \in \{1..M\} \tag{23}$$

where $\tau_m(t) = 1$ indicates that SC m is active at $t, t+\Delta t$, whereas $\tau_m(t) = 0$ means SC m is in sleep mode to reduce power consumption.

B. WORK OFFLOADING OF MEC-SCS

Among the active MEC-SCs, work offloading should be achieved to optimize the resource utilization efficiency, meanwhile ensuring on-demand QoS requirements by SGUEs. Therefore, a real-time D2D MEC-SC based work offloading algorithm is proposed.

Suppose an SBS m gains transmit power $P_m(t)$, $m \in \{1 \ldots M\}$. The data rate of one active SGUE n towards SBS m is measured and referred as $\sigma_{mn}(t)$. The total data rate received by SBS m, thus, is derived based on $N_m'(t)$ determined in (21), as:

$$\sigma_m(t) = \sum\nolimits_{i\in\{1..N_m'(t)\}} \sigma_{mn}(t)\,\tau_m(t), \quad m \in \{1..M\} \tag{24}$$

Compared with the estimated $\tilde{\sigma}_m(M, L_m)$ in (8), $\sigma_m(t)$ reflects the on-demand data rate requirement of individual SGUEs in real-time. We still have to define the maximum data rate that SBS m can support, similar to (6)-(8):

$$\sigma_m^{max}(t) = \sum\nolimits_{n\in\{1..N_m'(t)\}} \sigma_{mn}^{max}(t), \quad m \in \{1..M\}, \ n \in \{1..N\} \tag{25}$$

$$\sigma_{mn}^{max}(t) = B_m \log_2\left(1 + \frac{P_m(t)\cdot G_{mn}}{N + I_{mn}(t)} \cdot c_{mn}(t)\cdot a_{mn}(t)\right), \quad m \in \{1..M\}, \ n \in \{1..N\} \tag{26}$$

where

$$I_{mn}(t) = \sum\nolimits_{i\in\{1..M\}, i\neq m} \left[\mathbb{E}\left[P_i(t)\cdot G_{in}\cdot h_{in}(t)\right]\cdot\varphi_m(t)\right] \tag{27}$$

When SGUE o offloads its data to SGUE n via D2D with $\theta_{no}(t)$ defined in (2), the constraint for the data rate capacity of SGUE n should be fulfilled as:

$$\sum\nolimits_{m\in\{1..M\}}\left[\sigma_{mo}(t)\cdot\theta_{no}(t)+\sigma_{mn}(t)\right]\cdot a_{mn}(t) \le \sum\nolimits_{m\in\{1..M\}}\left[\sigma_{mn}^{max}(t)\cdot a_{mn}(t)\right],\quad \forall n,o\in\{1..N\} \tag{28}$$

In this paper, we focus on the work offloading among MEC-SCs, by assuming that the total computation capacity of MEC-SCs ($\sum_{m\in\{1..M\}}\varphi_m$, φ_m defined as the computation capacity of MEC-SC m) is capable of processing the workload of SGUEs. Cloud mainly acts as the central controller for the work offloading management among MEC-SCs to achieve global optimum, with data offloading to cloud targeted as our future work.

Therefore, similar to (2) and (4), we derive the data offloaded from MEC-SC m to MEC-SC q as

$$\theta_{mq}^{MEC-SC}(t) = \min\left\{\vartheta_m^{MEC-SC}(t),\vartheta_q^{MEC-SC}(t)\right\} = \begin{cases}1, & activated\\ 0, & otherwise,\end{cases} \quad m,q\in\{1..M\} \tag{29}$$

$$\forall\vartheta_m^{MEC-SC}(t)=1:\sum\nolimits_{q\in\{1..M\}}\theta_{mq}^{MEC-SC}(t)=1,\quad m,q\in\{1..M\} \tag{30}$$

The corresponding data offloaded from MEC-SC m to MEC-SC q at time t is defined as $\vec{\varphi}_{mq}(t)\in[-\varphi^{max},+\varphi^{max}]$, which should be limited according to the offloading capacity of HSCN. Besides, according to the consistency of the traffic, $\vec{\varphi}_{mq}(t)$ should be constrained as:

$$\forall\in m,q\in\{1..M\}:\vec{\varphi}_{mq}(t)+\vec{\varphi}_{qm}(t)=0,\quad m,q\in\{1..M\} \tag{31}$$

The overall workload by MEC-SC m, thus, is calculated as:

$$\sigma_m^{all}(t)=\sigma_m(t)+\sum\nolimits_{q\in\{1..M\}}\vec{\varphi}_{mq}(t)\cdot\theta_{mq}^{MEC-SC}(t)\le\varphi_m \tag{32}$$

The overall computation latency is further calculated, based on M/M/1 queuing system [35], as:

$$D_{cp}^{MEC-SC}(t)=\sum\nolimits_{m\in\{1..M\}}\frac{1}{\varphi_m-\sigma_m^{all}(t)} \tag{33}$$

where the computation power consumption is linearized with power consumption for unit data processing ε [35]:

$$E_{cp}^{MEC-SC}(t)=\sum\nolimits_{m\in\{1..M\}}\left[\varepsilon\cdot\sigma_m^{all}(t)\right] \tag{34}$$

It is necessary to notice here that the communication latency among SGUE-SC is determined by the k-means clustering based SC powering discussed in Section V.A. This subsection mainly aims to minimize the computation latency of MEC-SCs:

$$\min_{\vec{\varphi}_{mq}(t),m,q\in\{1..M\}} D_{cp}^{MEC-SC}(t) \tag{35}$$

$$\text{s.t. (28), (32)},$$

$$E_{cp}^{MEC-SC}(t)\le E_{cp,max}^{MEC-SC} \tag{36}$$

$$\vec{\varphi}_{mq}(t)\in\left[-\varphi^{max},+\varphi^{max}\right] \tag{37}$$

Equation (35) (inverse proportional function) can be solved by optimizing the equivalent augmented Lagrangian objective function, with Lagrangian multipliers and penalty terms as (38), as shown at the bottom of the page.

$\alpha_1(t)$ to $\alpha_3(t)$ are the Lagrangian multipliers for the constraints. $D_{cp}^{MEC-SC}(t)$, regarding $\vec{\varphi}_{mq}(t)$, is an inverse proportional function. Equation (28) can be achieved by optimal link budget in spatial SC allocation. Besides, it is intuitive that (36) and (37) are linear constraints. Therefore, the optimization problem can be solved by the iterative gradient descent method, given its fast convergence and global optimum ensured, which updates the controllable variable, $\vec{\varphi}_{mq}(t), m,q\in\{1..M\}$ to the opposite direction of the gradient in the solution space. Lagrangian multipliers are also updated iteratively with the principle in (39)-(40), as shown at the bottom of the page.

Ω_j is the corresponding penalty term for α_j (e.g., $E_{cp}^{MEC-SC}(t)-E_{cp,max}^{MEC-SC}$ for α_1). v should be determined

$$\min_{\vec{\varphi}_{mq}(t),m,q\in\{1..M\}} D_{cp}^{MEC-SC}(t)+\alpha_1(t)\left(E_{cp}^{MEC-SC}(t)-E_{cp,max}^{MEC-SC}\right)+\alpha_2(t)\left(\vec{\varphi}_{mq}(t)-\varphi^{max}\right)^2 +\alpha_3(t)\left(\sigma_m(t)+\sum\nolimits_{q\in\{1..M\}}\vec{\varphi}_{mq}(t)\cdot\theta_{mq}^{MEC-SC}(t)-\varphi_m\right) \tag{38}$$

$$m,q\in\{1..M\}:\vec{\varphi}_{mq}^{\,i+1}(t) = \vec{\varphi}_{mq}^{\,i}(t)-v\cdot\left(\frac{\theta_{mq}^{MEC-SC}(t)}{\left[\varphi_m-\left(\sigma_m(t)+\sum_{q\in\{1..M\}}\vec{\varphi}_{mq}^{\,i}(t)\cdot\theta_{mq}^{MEC-SC}(t)\right)\right]^2}+\alpha_1^i(t)\cdot\varepsilon\cdot\theta_{mq}^{MEC-SC}(t)+2\alpha_2^i(t)\cdot\vec{\varphi}_{mq}^{\,i}(t)+\alpha_3^i(t)\cdot\theta_{mq}^{MEC-SC}(t)\right) \tag{39}$$

$$\alpha_j^{i+1}(t)=\alpha_1^i(t)-v\cdot\Omega_j,\quad j\in\{1,2,3\} \tag{40}$$

TABLE 3. Operation flow of TOPSO.

TOPSO

%% Input

SGUE: $\{S_i, L_n, G_n\}, i \in \{g, r, l, e\}, n \in \{1..N\}$;

SGUE - MEC-SC: $\{\vartheta_n(t), c_{mn}(t), a_{mn}(t)\}, m \in \{1..M\}, n \in \{1..N\}$;

MEC-SC: $\{M^{optimal}, L_{M^{optimal}}\}$;

1. $t = 0$;

%% MEC-SC powering strategy

2. *Get*: periodic and non-periodic SGUEs: $\{N_m^{p\prime}(t), N_m^{np\prime}(t)\}$;

% k-means clustering based SGUE grouping

3. $i = 0$;

4. *Set*: adequate partition number by hard splitting into K groups

5. Select randomly k elements and assign as the cluster centroids $\mu_k^i(t)$

6. Assign all the remaining elements to a cluster with min. distance to the center based on power system layer

$$\arg\min_{k\in\{1..K\}} \left\| L_n - L^i_{\mu_k^i(t)} \right\|^2 n \in \{1..(N_m^{p\prime}(t) + N_m^{np\prime}(t))\};$$

7. $i = i+1$;

8. *Update*: $\mu_k^i(t)$;

9. *Repeat*: Step 4, *until* {"No SGUE re-assigned", $\mu_k^i(t) = \mu_k^{i-1}(t), k \in \{1..K\}, i = i_{max}\}$;

% Output: $\tau_m(t), m \in \{1..M\}$

%% MEC-SC offloading

10. *Get*: $\{\sigma_m(t), \sigma_m^{max}(t), \varphi_m\}, m \in \{1..M\}$

11. *Set*: optimization function and constraints (35)-(37), solving: $\vec{\varphi}_{mq}(t), m, q \in \{1..M\}$;

12. Lagrangian modeling: solving $\{\vec{\varphi}_{mq}(t), \alpha_1(t), \alpha_2(t), \alpha_3(t)\}, m, q \in \{1..M\}$;

13. $i = 1$;

14. Updating $\{\vec{\varphi}_{mq}^{i+1}(t), \alpha_j^{i+1}(t)\}, j \in \{1,2,3\}, m, q \in \{1..M\}$, according to gradient descent (39)-(40);

15. $i = i+1$;

16. *Repeat*: Step 15;

17. *Output*: $\vec{\varphi}_{mq}^{i+1}(t), m, q \in \{1..M\}$, optimal $\{D_{cp}^{MEC-SC}(t), E_{cp}^{MEC-SC}(t)\}$

18. $t = t+1$;

19. *Repeat:* Step 2;

to be small enough to ensure the convergence to the saddle point of the Lagrangian. The gradient descent based on-demand MEC-SC offloading gains sufficient computation latency with low complexity, which fulfill the real-time SC deployment for microgrids.

Operation flow of TOPSO is summarized in TABLE 3. After obtaining features of SGUEs, SGUE-SC association, and MEC-SCs, TOPSO adopts k-means clustering to group active SGUEs $(N_m^{p\prime}(t) + N_m^{np\prime}(t))$ into determined K groups. Cluster centroids $\mu_k^i(t)$ is updated iterationally, until the assignment all the SGUEs and cluster centroids are converged, or the maximum iteration is reached. Sleeping strategy based MEC-SC powering, then, outputs the activated MEC-SCs $(\tau_m(t), m \in \{1..M\})$, determined by the coverage of centroids of clusters $(\mu_k^{i_{max}}(t))$. Since some MEC-SCs sleep according to MEC-SC powering strategy, as well as SGUEs are allocated/operated heterogeneously, MEC-SC offloading is conducted by TOPSO, by formulating energy-aware overall computation latency optimization by Lagrangian modeling. Gradient descent based algorithm is developed, given its fast convergence and simplified computation. Real-time MEC-SC offloading outputs the guidance of offloading $(\vec{\varphi}_{mq}^{i+1}(t), m, q \in \{1..M\})$, which achieves minimized $D_{cp}^{MEC-SC}(t)$ with optimal $E_{cp}^{MEC-SC}(t)$.

VI. PERFORMANCE ANALYSIS

In this section, we develop three-step performance analysis to evaluate the proposed 3xSD, systemically and convincingly. Step 1 analyzes the long-term energy efficiency and achievable QoS improvement by the proposed SC positioning scheme, which will be discussed in Section VI.A. Following Step 1, Step 2 showcases the dynamic latency performance and energy efficiency optimization of TOSPO for different scales of microgrid, shown in Section VI.B. Step 3 evaluates the overall performance of the proposed 3xSD on the case study with IEEE 342-Node system (a typical test feeder for microgrids [43]) and selected benchmarks.

A. SPATIAL ANALYSIS OF THE SPATIAL SC POSITIONING SCHEME

This subsection is devoted to the evaluation of the proposed SC positioning scheme. Scenarios with multiple scales of microgrids with the number of SGUEs varied in the range: $N = \{200, 400, 600\}$ are considered, where the proposed spatial SC positioning scheme provides optimal number of SCs with their positioning. With the typical radius of MBSs (1km) and SBSs (0.2km) [35], it is not hard to determine that the maximum number of SBSs in each MBS is ~25, to prevent serious inter-SC interference.

Figure 2(a)-(c) shows the three criterions (normalized, i.e., achievable data rate $(\tilde{\sigma})$, energy efficiency $(\tilde{E})$, and interference mitigation $(\tilde{\gamma})$) for the designed three scenarios $(N = \{200, 400, 600\})$, respectively. Generally, $\tilde{\sigma}$ is proportional to M for all scales, resulting in higher efficiency of spectrum utilization. $\tilde{E}$ is improved at first and then drops down after the peak value, regarding the increase of M. Smaller M might fail to provide sufficient data rate $(\tilde{\sigma})$ to SGUEs, whereas excessive M results in unnecessary power consumption and cost. Therefore, $\tilde{E}$ achieves its peak value when $M = \{5,10,13\}$ for $N = \{200,400,600\}$, respectively. Similarly, $\tilde{\gamma}_m$ gains its peak value at $M = \{7,15,21\}$ for $N = \{200,400,600\}$, respectively, rendering insufficient SBSs losing coverage of SGUEs located at the edge of MBSs and excessive SCs potentially causing serious inter-SC interference.

It is obvious that trade-off solution should be determined when considering the three criterions $(\tilde{\sigma}, \tilde{E}, \tilde{\gamma})$ simultaneously, which achieves optimum on different M in the solution space. Therefore, Figure 3(a)-(i) represents the achievement of $\tilde{\sigma}, \tilde{E}, \tilde{\gamma}$ for different scales with varying weightings by the proposed SC positioning scheme, respectively. Based on (10), $\{\omega_1, \omega_2, \omega_3\}$ represents the weighting coefficient for $\tilde{\sigma}, \tilde{E}, \tilde{\gamma}$, respectively, with ω_1 plotted on x-axis and ω_2 on y-axis. ω_3 can be simply obtained by $\omega_3 = 1 - \omega_1 - \omega_2$.

In general, each criterion can achieve better performance with its corresponding weighting as higher. For instance, $\tilde{\sigma}$ increases linearly with the increasing of its weighting coefficient (ω_1). Similar principles occur to $\tilde{E}/\omega_2$ and $\tilde{\gamma}/\omega_3$, respectively. Besides, the reduction of $\tilde{\sigma}$ could deteriorate $\tilde{E}$, due to the definition of $\tilde{E}$ in this paper as "bit/J/Hz". Based

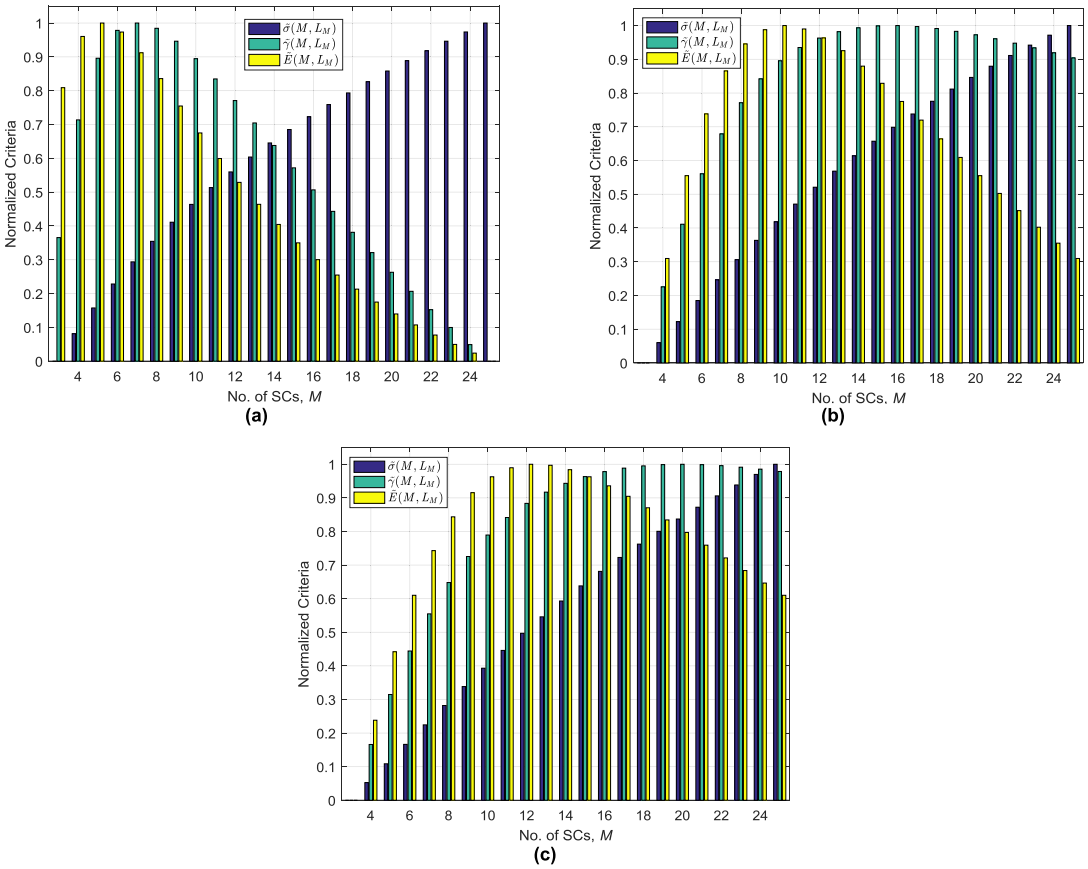

FIGURE 2. The main criterions (normalized) vs. No. of SCs for (a) $N = 200$; (b) $N = 400$; (c) $N = 600$.

on Figure 3, the proposed spatial SC positioning scheme provides guidance to the spatial SC deployment with long-term ($\tilde{\sigma}$, $\tilde{E}$, $\tilde{\gamma}$) optimization. The peak value of $\tilde{\sigma}$, $\tilde{E}$, $\tilde{\gamma}$ can be potentially achieved as {21.14, 64.82, 93.89}Mbps, {8.92, 23.68, 30.75}bit/J/Hz, and {20.52, 23.91, 29.45}dB for $N = \{200, 400, 600\}$, respectively. With $\omega_1 = \omega_2 = \omega_3$ representing a generic case, the average $\tilde{\sigma}$, $\tilde{E}$, $\tilde{\gamma}$ achieves {18.01, 44.96, 73.55}Mbps, {8.88, 23.66, 30.65}bit/J/Hz and {19.99, 22.46, 28.78}dB for $N = \{200, 400, 600\}$, respectively, with $M = \{5, 11, 14\}$.

B. DYNAMIC ANALYSIS OF TOSPO

This subsection discusses the dynamic on-demand HSCN deployment by the proposed TOSPO (powering and work offloading), for different scales of microgrid based smart grid. Features of SGUEs are randomly assigned with S_i, L_n, C_n, $tr_n(t)$, $\vartheta_n(t)$, $\theta_{no}(t)$, $c_{mn}(t)$ and $a_{mn}(t)$. TOSPO is evaluated within 60 sec, with time interval as 1 sec. To reflect the concern of privacy of SGUEs, probability of D2D is assigned as [0,0.8] if SGUEs are clustered in the same microgrid, and [0,0.2] otherwise. Intuitively, With the increase of D2D probability, the data rate of the whole system increases near-linearly [3].

Figure 4 shows the real-time $D_{cp}^{MEC-SC}(t)$ and the corresponding required workload ($\sigma(t)$), during the operation time. Generally, $D_{cp}^{MEC-SC}(t)$ is proportional to the required $\sigma(t)$, with limited computation power of MEC-SCs. Although SGUEs are located randomly and operated dynamically, the proposed TOSPO is capable of covering all the SGUEs and providing efficient computation capacity with computation latency less than 22.73sec for $N \leq 600$. Moreover, the difference between the average $D_{cp}^{MEC-SC}(t)$ for different microgrid scales in Figure 4 (a) limits to ∼0.23%, indicating the high scalability with stable performance of the proposed TOSPO. For instance, since M for $N = \{200, 400, 600\}$ is obtained by the spatial SC positioning scheme as $M = \{5, 11, 14\}$, respectively, the influence on the average $D_{cp}^{MEC-SC}(t)$ by different microgrid scales limits within ∼0.3ms/MEC-SC, which potentially supports microgrid with ultra-dense MEC-SCs.

Moreover, generally, shown in Figure 4 (a), without D2D activated, $D_{cp}^{MEC-SC}(t)$ increases, due to the increased data aggregation in MEC-SCs, based on (24), (32)-(33). On average, based on the D2D probability determined in TABLE 4, $D_{cp}^{MEC-SC}(t)$ can be improved by 11.59% with D2D activated.

Figure 5 shows the MATLAB based convergence time of the proposed TOSPO, operated on i7-4702MQ CPU and 8GB RAM. Concretely, since the fast convergence of gradient descent based algorithm, the work offloading algorithm achieves an average of 4.14ms, with variance less than 0.59 for $N = \{200, 400, 600\}$. The k-means clustering

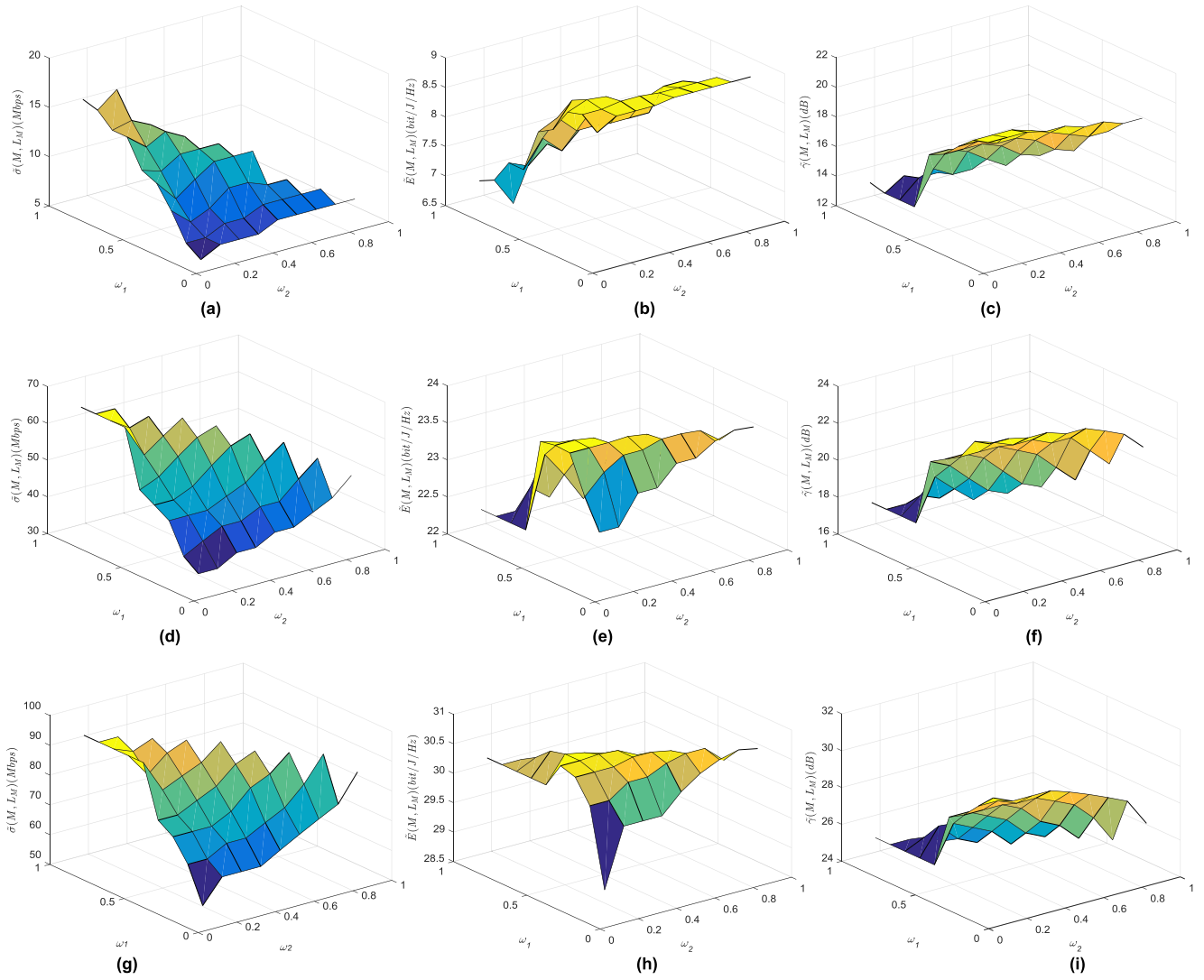

FIGURE 3. Optimal $\tilde{\sigma}, \tilde{E}, \tilde{\gamma}$ with varying $\omega_1, \omega_2, \omega_3$ for $N = \{200,400,600\}$: (a) Optimal $\tilde{\sigma}$ for $N = 200$; (b) Optimal $\tilde{E}$ for $N = 200$; (c) Optimal $\tilde{\gamma}$ for $N = 200$; (d) Optimal $\tilde{\sigma}$ for $N = 400$; (e) Optimal E for $N = 400$; (f) Optimal $\tilde{\gamma}$ for $N = 400$; (g) Optimal $\tilde{\sigma}$ for $N = 600$; (h) Optimal E for $N = 600$; (i) Optimal $\tilde{\gamma}$ for $N = 600$.

proposed SC powering algorithm also performs acceptable convergence with the maximum convergence time for $N = 600$ as 20.22ms. Therefore, the overall achieved convergence time of TOSPO is as small as 25.08ms, sufficient to support microgrids [44].

C. CASE STUDY OF THE PROPOSED 3xSD

In this subsection, a typical test feeder for communication system analysis in microgrids, IEEE 342-Node system, is selected as the testbed. Parameter settings for the case study are based on the setup of IEEE 342-Node system, shown in TABLE 4. To showcase the performance of the proposed 3xSD, two benchmarks, representative of the advanced HSCN deployment, are selected to represent the spatial and temporal benchmarks respectively, which include:

1. Optimization of D2D-based data rate optimization and interference mitigation (ODDRI) [3], which focuses on SC positioning, with D2D probability estimated during the initialization of HSCNs.

2. Dynamic MEC-SC offloading based on ADMM (ADMM-MEC-SC) [35], which aims to achieve low power consumption and low computation time by real-time offloading algorithm.

Suppose half of SGUEs transmit data periodically, and the rest non-periodically in time $t \in [0, 60]$ sec with $\Delta t = 1$ sec. SGUEs are located based on the Poisson distribution, with the distance between each other ranging in [0,24] m, as indicated in IEEE 342-Node system. Besides, the packet size is designed as [256, 1024] bits to reflect the practical demand of SGUEs.

Based on the parameter settings in the case study, the proposed spatial SC positioning scheme in 3xSD is activated to initialize the HSCN, with the corresponding $M = 14$ with $\omega_1 = \omega_2 = \omega_3$, as aforementioned in Section VI.B. Therefore, based on the dynamic SGUEs

TABLE 4. Parameter setting of dynamic simulation analysis.

Parameters	Note
No. of SGUEs	628
No. of periodic/non-periodic SGUEs	{314,314}
Radius (m) of Macro-cells	1000
Radius (m) of SCs	200
UE-UE distance (m)	[0,24]
D2D probability (inter-Microgrids)	[0,0.2]
D2D probability (inner-Microgrid)	[0,0.8]
Time interval/operation (sec)	1
Total operation time (sec)	60
Packet size (bits)	[256,1024]
$\delta_{tr_n(t)=0}(t), \delta_{tr_n(t)=1}(t)$	[0,1]

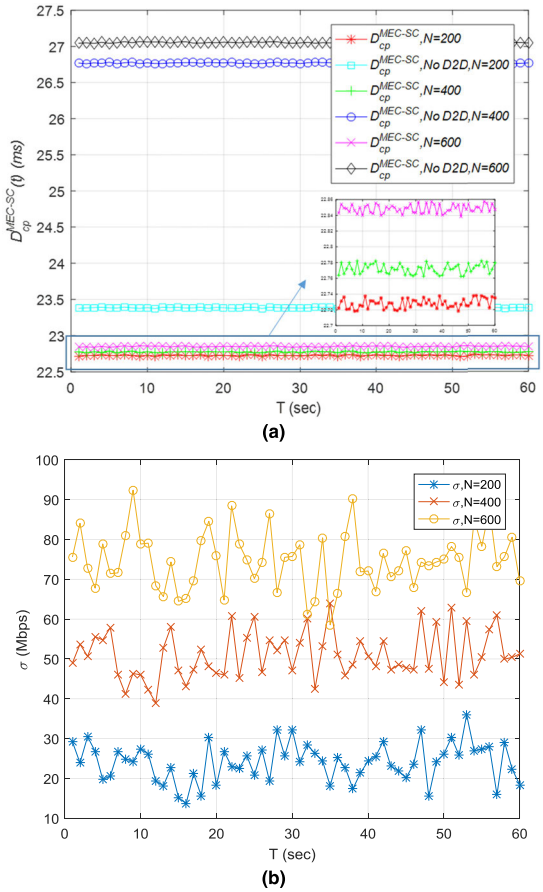

FIGURE 4. (a) $D_{cp}^{MEC-SC}(t)$; (b) required dynamic $\sigma(t)$ required by SGUEs vs. operation time.

operation pattern, the initialized SC positioning and powering within one macro-cell at $t = 0$ is shown in Figure 6. According to the operation patterns of SGUEs at $t = 0$, k-means clustering based SC powering in TOSPO determines the sleeping modes for SCs, as shown in Figure 6, by which the active SCs can cover all the cluster centroids obtained by TOSPO, with D2D.

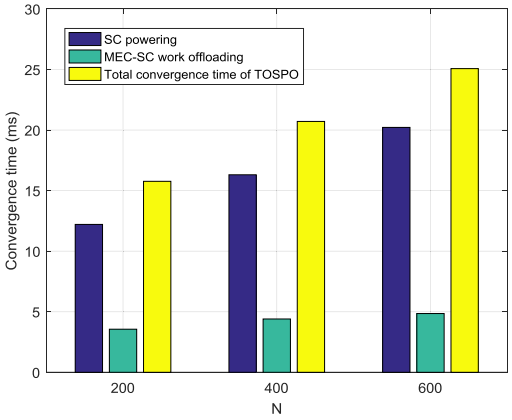

FIGURE 5. Computation convergence latency of TOSPO (powering + offloading).

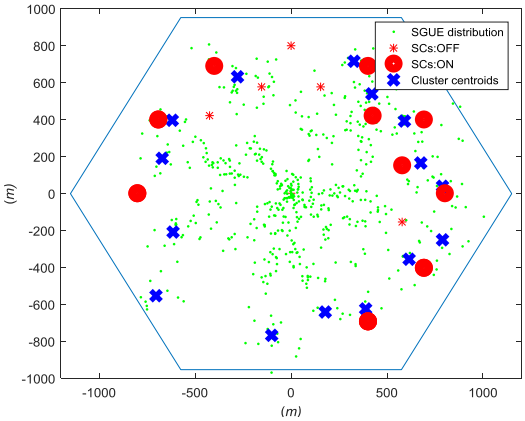

FIGURE 6. HSCN deployment (SC positioning and powering) (t=0).

Figure 7 shows the real-time total latency during the operation. After initialization ($t < 2$ sec), the convergence time of the proposed 3xSD limits to [21.94, 23.52] ms, whereas the communication and computation latency of 3xSD is relatively stabilized in the range of [37.85, 41.65] ms. Similarly, the benchmark ODDRI requires a larger latency for initializing the HSCN for microgrid. However, since real-time work offloading is lacked, the latency of ODDRI deteriorates during the operation, with the accumulation of the excessive workload of busy MEC-SC, while leaving certain less-heavy-load MEC-SCs idle. On the other hand, ADMM-SC could achieve the workload offloading among MEC-SCs, yet non-optimal MEC-SC positioning results in a larger latency up to 93.26ms. In summary, the average achieved latency of the proposed 3xSD during the operation reaches as lows as 60.18ms, which surpasses the benchmarks, ODDRI and ADDM-MEC-SC, by 27.81% and 35.47%, respectively.

Figure 8 depicts the energy efficiency ($E_{cp}^{MEC-SC}(t)$) of the proposed 3xSD within [0, 60] sec, compared to the two considered benchmarks. The fluctuation of $E_{cp}^{MEC-SC}(t)$ is consistent with the real-time data rate demanded by

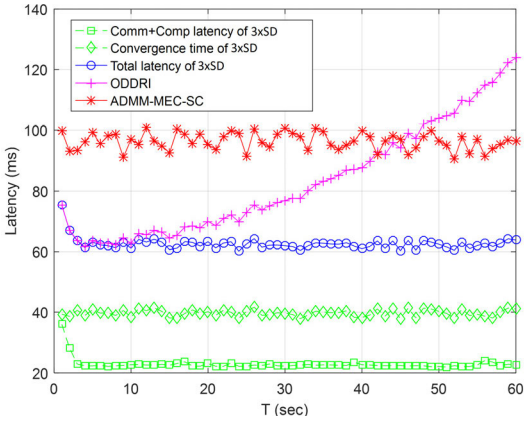

FIGURE 7. Latency performance of 3xSD and benchmarks.

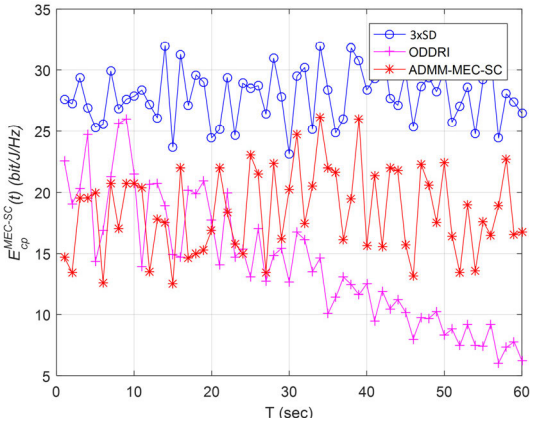

FIGURE 8. $E_{cp}^{MEC-SC}(t)$ of the proposed 3xSD.

SGUEs. Meanwhile, $E_{cp}^{MEC-SC}(t)$ can also be improved by the proposed 3xSD with SC powering. Similar to Figure 7, $E_{cp}^{MEC-SC}(t)$ of ODDRI decreases along operation time, rendering the deteriorated data rate because of the workload congestion. By contrast, the proposed 3xSD gains the stable outperformance on $E_{cp}^{MEC-SC}(t)$ optimization, with an average value of 27.90 bit/J/Hz, superior to the benchmarked ODDRI and ADDM-MSC-SC by 49.05% and 33.93%, respectively. Therefore, with the spatiotemporal HSCN deployment for microgrids, the proposed 3xSD achieves optimal latency and energy efficiency performance with high scalability and reliability, chronically and dynamically, which provides optimal energy efficient and QoS-ensured solution for large scale microgrids.

VII. CONCLUSION

This paper proposes a spatiotemporal D2D small cell allocation and on-demand deployment for Microgrid based smart grid development (MSD), named as 3xSD, which extracts the features of smart grid user equipment (SGUEs) chronically and dynamically, from both physical and cyber layers of microgrids. Concretely, a spatial small cell positioning algorithm is proposed based on VIKOR, which achieves optimal long-term achievable data rate and energy efficiency with interference mitigation. On top of the spatial SC positioning scheme, a temporal on-demand Small cell powering and work-offloading scheme (TOSPO) is proposed to maximize the real-time energy efficiency and minimize the overall latency, simultaneously, with the fusion of k-means clustering and gradient descent algorithm. The proposed 3xSD is evaluated with spatial analysis, temporal analysis, and case study based on a typical test feeder (IEEE 342-Node system). Numerical results indicate that the proposed 3xSD achieves energy efficiency and latency as 27.90 bit/J/Hz and 60.18 ms on average, outperforming the selected benchmarks, by at least 33.93% and 27.81%, respectively. Therefore, the proposed 3xSD provides a high energy-efficiency, high scalability and optimized latency solution, chronically and dynamically, for microgrid. We will further extend the proposed 3xSD towards larger scale smart grid development (e.g., city-wide, etc.), together with the resilience study regarding emergency handling, as future work.

REFERENCES

[1] T. V. Vu, B. L. H. Nguyen, Z. Cheng, M.-Y. Chow, and B. Zhang, "Cyber-physical microgrids: Toward future resilient communities," *IEEE Ind. Electron. Mag.*, vol. 14, no. 3, pp. 4–17, Sep. 2020, doi: 10.1109/MIE.2019.2958039.

[2] B. Cao, W. Dong, Z. Lv, Y. Gu, S. Singh, and P. Kumar, "Hybrid microgrid many-objective sizing optimization with fuzzy decision," *IEEE Trans. Fuzzy Syst.*, vol. 28, no. 11, pp. 2702–2710, Nov. 2020, doi: 10.1109/TFUZZ.2020.3026140.

[3] H. R. Chi, M. F. Domingues, A. Refaey, and A. Radwan, "Energy-efficient and QoS-improved D2D small cell deployment for smart grid," in *Proc. IEEE Global Commun. Conf. (GLOBECOM)*, Dec. 2020, pp. 1–6, doi: 10.1109/GLOBECOM42002.2020.9322108.

[4] S. Hu, X. Chen, W. Ni, X. Wang, and E. Hossain, "Modeling and analysis of energy harvesting and smart grid-powered wireless communication networks: A contemporary survey," *IEEE Trans. Green Commun. Netw.*, vol. 4, no. 2, pp. 461–496, Jun. 2020, doi: 10.1109/TGCN.2020.2988270.

[5] X. Xue, W. Sun, J. Wang, Q. Li, G. Luo, and K. Yu, "RVFL-LQP: RVFL-based link quality prediction of wireless sensor networks in smart grid," *IEEE Access*, vol. 8, pp. 7829–7841, 2020, doi: 10.1109/ACCESS.2020.2964319.

[6] H. R. Chi and A. Radwan, "Multi-objective optimization of green small cell allocation for IoT applications in smart city," *IEEE Access*, vol. 8, pp. 101903–101914, May 2020, doi: 10.1109/ACCESS.2020.2997761.

[7] A. R. Radwan, K. M. S. Huq, S. Mumtaz, K.-F. Tsang, and J. Rodriguez, "Low-cost on-demand C-RAN based mobile small-cells," *IEEE Access*, vol. 4, pp. 2331–2339, 2016, doi: 10.1109/ACCESS.2016.2563518.

[8] H. Zhang, Y. Wang, H. Ji, and X. Li, "A sleeping mechanism for cache-enabled small cell networks with energy harvesting function," *IEEE Trans. Green Commun. Netw.*, vol. 4, no. 2, pp. 497–505, Jun. 2020, doi: 10.1109/TGCN.2020.2988276.

[9] X. Chen, C. Wu, Z. Liu, N. Zhang, and Y. Ji, "Computation offloading in beyond 5G networks: A distributed learning framework and applications," *IEEE Wireless Commun.*, vol. 28, no. 2, pp. 56–62, Apr. 2021, doi: 10.1109/MWC.001.2000296.

[10] C. Feng, K. Yu, A. K. Bashir, Y. D. Al-Otaibi, Y. Lu, S. Chen, and D. Zhang, "Efficient and secure data sharing for 5G flying drones: A blockchain-enabled approach," *IEEE Netw.*, vol. 35, no. 1, pp. 130–137, Jan. 2021, doi: 10.1109/MNET.011.2000223.

[11] A.-E. M. Taha, N. A. Ali, H. R. Chi, and A. Radwan, "MEC resource offloading for QoE-aware HAS video streaming," presented at the ICC, Jun. 2021.

[12] T. Bai, C. Pan, Y. Deng, M. Elkashlan, A. Nallanathan, and L. Hanzo, "Latency minimization for intelligent reflecting surface aided mobile edge computing," *IEEE J. Sel. Areas Commun.*, vol. 38, no. 11, pp. 2666–2682, Nov. 2020, doi: 10.1109/JSAC.2020.3007035.

[13] Y. Zhang, B. Di, P. Wang, J. Lin, and L. Song, "HetMEC: Heterogeneous multi-layer mobile edge computing in the 6G era," *IEEE Trans. Veh. Technol.*, vol. 69, no. 4, pp. 4388–4400, Apr. 2020, doi: 10.1109/TVT.2020.2975559.

[14] X. Chen, C. Wu, T. Chen, H. Zhang, Z. Liu, Y. Zhang, and M. Bennis, "Age of information aware radio resource management in vehicular networks: A proactive deep reinforcement learning perspective," *IEEE Trans. Wireless Commun.*, vol. 19, no. 4, pp. 2268–2281, Apr. 2020, doi: 10.1109/TWC.2019.2963667.

[15] H. R. Chi and A. Radwan, "Integer-based multi-objective algorithm for small cell allocation optimization," *IEEE Commun. Lett.*, vol. 24, no. 11, pp. 2551–2554, Nov. 2020, doi: 10.1109/LCOMM.2020.3012013.

[16] C. Wu, Z. Liu, F. Liu, T. Yoshinaga, Y. Ji, and J. Li, "Collaborative learning of communication routes in edge-enabled multi-access vehicular environment," *IEEE Trans. Cognit. Commun. Netw.*, vol. 6, no. 4, pp. 1155–1165, Dec. 2020, doi: 10.1109/TCCN.2020.3002253.

[17] L. Nguyen, G. Hu, and C. J. Spanos, "Efficient sensor deployments for spatio-temporal environmental monitoring," *IEEE Trans. Syst., Man, Cybern. Syst.*, vol. 50, no. 12, pp. 5306–5316, Dec. 2020, doi: 10.1109/TSMC.2018.2872041.

[18] S. D. Okegbile, B. T. Maharaj, and A. S. Alfa, "Spatiotemporal characterization of users' experience in massive cognitive radio networks," *IEEE Access*, vol. 8, pp. 57114–57125, 2020, doi: 10.1109/ACCESS.2020.2981953.

[19] L. Chen, S. Zhou, and J. Xu, "Computation peer offloading for energy-constrained mobile edge computing in small-cell networks," *IEEE/ACM Trans. Netw.*, vol. 26, no. 4, pp. 1619–1632, Aug. 2018, doi: 10.1109/TNET.2018.2841758.

[20] I. F. Akyildiz, A. Kak, and S. Nie, "6G and beyond: The future of wireless communications systems," *IEEE Access*, vol. 8, pp. 133995–134030, 2020, doi: 10.1109/ACCESS.2020.3010896.

[21] K. Yu, Z. Guo, Y. Shen, W. Wang, J. C.-W. Lin, and T. Sato, "Secure artificial intelligence of things for implicit group recommendations," *IEEE Internet Things J.*, early access, May 12, 2021, doi: 10.1109/JIOT.2021.3079574.

[22] Z. Zhao, J. Guo, X. Luo, J. Xue, C. S. Lai, Z. Xu, and L. L. Lai, "Energy transaction for multi-microgrids and internal microgrid based on blockchain," *IEEE Access*, vol. 8, pp. 144362–144372, 2020, doi: 10.1109/ACCESS.2020.3014520.

[23] J. Duan and M.-Y. Chow, "Robust consensus-based distributed energy management for microgrids with packet losses tolerance," *IEEE Trans. Smart Grid*, vol. 11, no. 1, pp. 281–290, Jan. 2020, doi: 10.1109/TSG.2019.2921231.

[24] Z. Cheng, J. Duan, and M.-Y. Chow, "To centralize or to distribute: That is the question: A comparison of advanced microgrid management systems," *IEEE Ind. Electron. Mag.*, vol. 12, no. 1, pp. 6–24, Mar. 2018, doi: 10.1109/MIE.2018.2789926.

[25] K. Yu, L. Tan, L. Lin, X. Cheng, Z. Yi, and T. Sato, "Deep-learning-empowered breast cancer auxiliary diagnosis for 5GB remote E-health," *IEEE Wireless Commun.*, vol. 28, no. 3, pp. 54–61, Jun. 2021.

[26] H. Çimen, N. Çetinkaya, J. C. Vasquez, and J. M. Guerrero, "A microgrid energy management system based on non-intrusive load monitoring via multitask learning," *IEEE Trans. Smart Grid*, vol. 12, no. 2, pp. 977–987, Mar. 2021, doi: 10.1109/TSG.2020.3027491.

[27] H. Chen, H. Hui, Z. Su, D. Fang, and Y. Hui, "Real-time pricing strategy based on the stability of smart grid for green Internet of Things," *Mobile Inf. Syst.*, vol. 2017, pp. 1–11, Mar. 2017, doi: 10.1155/2017/5039702.

[28] A. M. Alqasir and A. E. Kamal, "Cooperative small cell HetNets with dynamic sleeping and energy harvesting," *IEEE Trans. Green Commun. Netw.*, vol. 4, no. 3, pp. 774–782, Sep. 2020, doi: 10.1109/TGCN.2020.2985496.

[29] F. A. Asuhaimi, S. Bu, and M. A. Imran, "Joint resource allocation and power control in heterogeneous cellular networks for smart grids," in *Proc. IEEE Global Commun. Conf. (GLOBECOM)*, Abu Dhabi, United Arab Emirates, Dec. 2018, pp. 1–6, doi: 10.1109/GLOCOM.2018.8647668.

[30] P. Trakas, F. Adelantado, N. Zorba, and C. Verikoukis, "A quality of experience-aware association algorithm for 5G heterogeneous networks," in *Proc. IEEE Int. Conf. Commun. (ICC)*, Paris, France, May 2017, pp. 1–6, doi: 10.1109/ICC.2017.7996869.

[31] Y. Wu, X. Yang, L. P. Qian, H. Zhou, X. Shen, and M. K. Awad, "Optimal dual-connectivity traffic offloading in energy-harvesting small-cell networks," *IEEE Trans. Green Commun. Netw.*, vol. 2, no. 4, pp. 1041–1058, Dec. 2018.

[32] R. Bonnefoi, C. Moy, and J. Palicot, "Power control and cell discontinuous transmission used as a means of decreasing small-cell networks' energy consumption," *IEEE Trans. Green Commun. Netw.*, vol. 2, no. 4, pp. 899–914, Dec. 2018, doi: 10.1109/TGCN.2018.2838759.

[33] A. A. Neghabi, N. J. Navimipour, M. Hosseinzadeh, and A. Rezaee, "Load balancing mechanisms in the software defined networks: A systematic and comprehensive review of the literature," *IEEE Access*, vol. 6, pp. 14159–14178, 2018, doi: 10.1109/ACCESS.2018.2805842.

[34] H. Chen, D. Zhao, Q. Chen, and R. Chai, "Joint computation offloading and radio resource allocations in small-cell wireless cellular networks," *IEEE Trans. Green Commun. Netw.*, vol. 4, no. 3, pp. 745–758, Sep. 2020.

[35] Y. Cheng, J. Zhang, L. Yang, C. Zhu, and H. Zhu, "Distributed green offloading and power optimization in virtualized small cell networks with mobile edge computing," *IEEE Trans. Green Commun. Netw.*, vol. 4, no. 1, pp. 69–82, Mar. 2020.

[36] M. Emara, H. ElSawy, M. C. Filippou, and G. Bauch, "Spatiotemporal dependable task execution services in MEC-enabled wireless systems," *IEEE Wireless Commun. Lett.*, vol. 10, no. 2, pp. 211–215, Feb. 2021, doi: 10.1109/LWC.2020.3024749.

[37] J. Wang, J. Tang, Z. Xu, Y. Wang, G. Xue, X. Zhang, and D. Yang, "Spatiotemporal modeling and prediction in cellular networks: A big data enabled deep learning approach," in *Proc. IEEE Conf. Comput. Commun. (INFOCOM)*, Atlanta, GA, USA, May 2017, pp. 1–9, doi: 10.1109/INFOCOM.2017.8057090.

[38] F. Benkhelifa, H. ElSawy, J. A. Mccann, and M.-S. Alouini, "Recycling cellular energy for self-sustainable IoT networks: A spatiotemporal study," *IEEE Trans. Wireless Commun.*, vol. 19, no. 4, pp. 2699–2712, Apr. 2020, doi: 10.1109/TWC.2020.2967697.

[39] Y. Zhong, T. Q. S. Quek, and X. Ge, "Heterogeneous cellular networks with spatio-temporal traffic: Delay analysis and scheduling," *IEEE J. Sel. Areas Commun.*, vol. 35, no. 6, pp. 1373–1386, Jun. 2017, doi: 10.1109/JSAC.2017.2687379.

[40] H. H. Yang and T. Q. S. Quek, "Spatio-temporal analysis for SINR coverage in small cell networks," *IEEE Trans. Commun.*, vol. 67, no. 8, pp. 5520–5531, Aug. 2019, doi: 10.1109/TCOMM.2019.2915832.

[41] M. Rana, L. Li, and S. W. Su, "Distributed state estimation over unreliable communication networks with an application to smart grids," *IEEE Trans. Green Commun. Netw.*, vol. 1, no. 1, pp. 89–96, Mar. 2017, doi: 10.1109/TGCN.2017.2675542.

[42] K. F. Tsang, H. R. Chi, L. Fu, L. Pan, and H. F. Chan, "Energy-saving IAQ monitoring ZigBee network using VIKOR decision making method," in *Proc. IEEE Int. Conf. Ind. Technol. (ICIT)*, Taipei, Taiwan, Mar. 2016, pp. 2004–2009, doi: 10.1109/ICIT.2016.7475075.

[43] K. Schneider, P. Phanivong, and J.-S. Lacroix, "IEEE 342-node low voltage networked test system," in *Proc. IEEE PES Gen. Meeting | Conf. Expo.*, Jul. 2014, pp. 1–5, doi: 10.1109/PESGM.2014.6939794.

[44] F. A. Asuhaimi, S. Bu, J. P. B. Nadas, and M. A. Imran, "Delay-aware energy-efficient joint power control and mode selection in device-to-device communications for FREEDM systems in smart grids," *IEEE Access*, vol. 7, pp. 87369–87381, 2019, doi: 10.1109/ACCESS.2019.2924488.

HAO RAN CHI (Member, IEEE) received the B.E. (Hons.) and Ph.D. degrees in electronic engineering from the City University of Hong Kong, in 2013 and 2018, respectively. He worked as a Postdoctoral Fellow with the City University of Hong Kong. He was also invited as a Visiting Scholar at the North Carolina State University, NC, USA, in 2019. He is currently a Researcher with the Instituto de Telecomunicações, Universidade de Aveiro, Portugal. His research interests include 5G, the IoT infrastructure development, wireless communication, evolutionary optimization, and machine learning.

MARIA DE FÁTIMA DOMINGUES (Member, IEEE) received the Ph.D. degree in physics engineering from the University of Aveiro, Portugal, in 2014. She is currently a Researcher with the Instituto de Telecomunicações, University of Aveiro. She has authored and coauthored more than 80 journal articles and conference papers, chapters, and books. Her current research interests embrace new solutions of optical fiber based sensors and its application in e-Health scenarios, with a focus in physical rehabilitation architectures.

KONSTANTIN. I. KOSTROMITIN received the bachelor's and master's degrees in physics with specialization in chair physics of condensed matter and the Ph.D. degree from Chelyabinsk State University, Chelyabinsk, Russia, in 2008, 2010, and 2013, respectively, and the degree (Hons.) in physics from the Department of Physical Education, Municipal Secondary School, Chelyabinsk State University, where he has completed the Ph.D. thesis entitled "Researching of Magnetocaloric Effect in Antiferromagnetics and Twins Moving in Heusler alloys" with specialization in physics of condensed matter in the Dissertation Council, in 2013.

AHMAD ALMOGREN (Senior Member, IEEE) received the Ph.D. degree in computer science from Southern Methodist University, Dallas, TX, USA, in 2002. He worked as the Vice Dean of the development and quality at CCIS. He is currently a Professor with the Department of Computer Science, College of Computer and Information Sciences (CCIS), King Saud University (KSU), Riyadh, Saudi Arabia, where he is also the Director of the Cyber Security Chair, CCIS. He also served as the Dean for the College of Computer and Information Sciences and the Head for the Academic Accreditation Council, Al Yamamah University. His research interests include mobile-pervasive computing and cyber security. He served as the General Chair for the IEEE Smart World Symposium and a Technical Program Committee Member for numerous international conferences/workshops, such as IEEE CCNC, ACM BodyNets, and IEEE HPCC.

AYMAN RADWAN (Senior Member, IEEE) received the M.A.Sc. degree from Carleton University, Ottawa, ON, Canada, and the Ph.D. degree from Queen's University, Kingston, ON, Canada, in 2009. He has worked for a year at Queen's University, as a Research Assistant, before moving to Portugal, in January 2010. In January 2010, he joined the Instituto de Telecomunicações as a Senior Researcher and to help with EU project coordination and technical management. Since then, he has been intensively active in European projects, coordinating and technically managing multiple EU projects. He acted as the Technical Manager of the FP7 Project C2POWER (ten partners and Budget: e5M). He was also the Coordinator of the CELTIC Project Green-T (17 partners and Budget: e6.5M) and the CELTIC Plus project MUSCLES (six partners and Budget: e4.5M). He has just managed to secure a new project CELTIC-NEXT SAFE-HOME, with a budget of e8M (26 partners). He has an extensive experience in coordinating and managing collaborative projects at EU and International level, with multiple millions Euros budget. He previously participated in ETN Greenet as a Mentor for ESRs and was with the Management Team of ITN-SECRET, in February 2019. He is also supervising multiple Ph.D. students and Postdoctoral Fellows. He has authored more than 120 scientific works in the field of wireless networks, with emphasis on future generations of mobile communications, virtualization, RRM, and efficient networking for the IoT. He has also authored two books and four patents. He is an Associate Editor of the IEEE COMMUNICATIONS LETTERS and the *IEEE Network Magazine*.